Inter-Landau-level Andreev Reflection at the Dirac Point in a Graphene Quantum Hall State Coupled to a $NbSe_2$ Superconductor

Manas Ranjan Sahu,[1] Xin Liu,[2] Arup Kumar Paul,[1] Sourin Das,[3] Pratap Raychaudhuri,[4] J. K. Jain,[5] and Anindya Das[1,*]
[1]Department of Physics, Indian Institute of Science, Bangalore 560012, India
[2]School of Physics, Huazhong University of Science and Technology, Wuhan 430074, China
[3]Indian Institute of Science Education and Research, Kolkata, Mohanpur 741246, India
[4]Tata Institute of Fundamental Research, Homi Bhabha Road, Colaba, Mumbai 400 005, India
[5]Department of Physics, The Pennsylvania State University, University Park, Pennsylvania 16802, USA

(Received 11 December 2017; published 24 August 2018)

Superconductivity and the quantum Hall effect are distinct states of matter occurring in apparently incompatible physical conditions. Recent theoretical developments suggest that the coupling of the quantum Hall effect with a superconductor can provide fertile ground for realizing exotic topological excitations such as non-Abelian Majorana fermions or Fibonacci particles. As a step toward that goal, we report observation of Andreev reflection at the junction of a quantum Hall edge state in a single layer graphene and a quasi-two-dimensional niobium diselenide ($NbSe_2$) superconductor. Our principal finding is the observation of an anomalous finite-temperature conductance peak located precisely at the Dirac point, providing a definitive evidence for inter-Landau-level Andreev reflection in a quantum Hall system. Our observations are well supported by detailed numerical simulations, which offer additional insight into the role of the edge states in Andreev physics. This study paves the way for investigating analogous Andreev reflection in a fractional quantum Hall system coupled to a superconductor to realize exotic quasiparticles.

DOI: 10.1103/PhysRevLett.121.086809

The proximity effect through Andreev reflection (AR) is the primary ingredient for engineering a topological superconductor, which is expected to be a breeding ground for new types of topological excitations [1–8]. Discovery of graphene in the last decade [9], aided by developments in improving device quality by encapsulating with hexagonal boron nitride [10,11] (hBN), provides one of the best opportunities to extend the study of AR for Dirac electrons in proximity to superconductors [12–19]. In these systems an incident electron from single layer graphene (SLG) with a finite excitation energy combines with another electron below the Fermi energy (E_F) to form a Cooper pair at the junction [Fig. 1(a), top]. The AR and its transition from retro to nonretro reflection has been observed [17]. More interestingly, when E_F is aligned with the Dirac point, AR requires an interband process and is predicted to be specular [Fig. 1(a), top], as observed recently in bilayer graphene [16].

Exotic physics is predicted to arise from the coupling between a superconductor and a topological quantum Hall (QH) state. In particular, this system has been proposed as a novel route for creating a variety of non-Abelian anyons, which have been hailed as possible building blocks for future topological quantum computation [6,20,21]. The physics of AR is predicted to alter dramatically in the QH regime [22–24], where electron transport occurs primarily through the chiral edge states, which themselves are topologically robust manifestations of the Landau Levels (LLs) in the interior of the sample. On the QH plateau, an incident chiral electron is expected to bounce back as an Andreev-reflected chiral hole propagating in the same direction as the incoming electron [Fig. 1(a), bottom] [25], due to the sign reversals of both the charge and the mass. A difficulty in experimentally investigating this physics is the fact that high magnetic fields required for the QH effect are inimical to superconductivity. Important progress has recently been made in this direction. Supercurrent and Josephson coupling in QH regime at the SLG-superconductor interface have been demonstrated at relatively low magnetic field (∼2 T) [26–28]. At high magnetic fields (∼10 T) the superconducting correlations in QH edge has been realized recently [29].

In this work, we show that a coexistence of, and a coupling between, a QH system and a superconductor can be realized and studied in a system of SLG coupled to a $NbSe_2$ superconductor. Our results reveal that at high magnetic fields, when the breaking of the spin and valley symmetries generally fully splits the zeroth Landau level [30–32], AR manifests most strikingly through an anomalous conductance peak located precisely at the Dirac point (DP). We attribute this peak to inter-Landau-level AR, and confirm its physical origin by detailed theoretical simulations.

Our devices consist of an SLG partially covered with a thin film of $NbSe_2$ [Fig. 1(b)]. Details of the fabrication and measurement schemes are given in the Supplemental Material [33], Sec. SI1. We show results from three devices

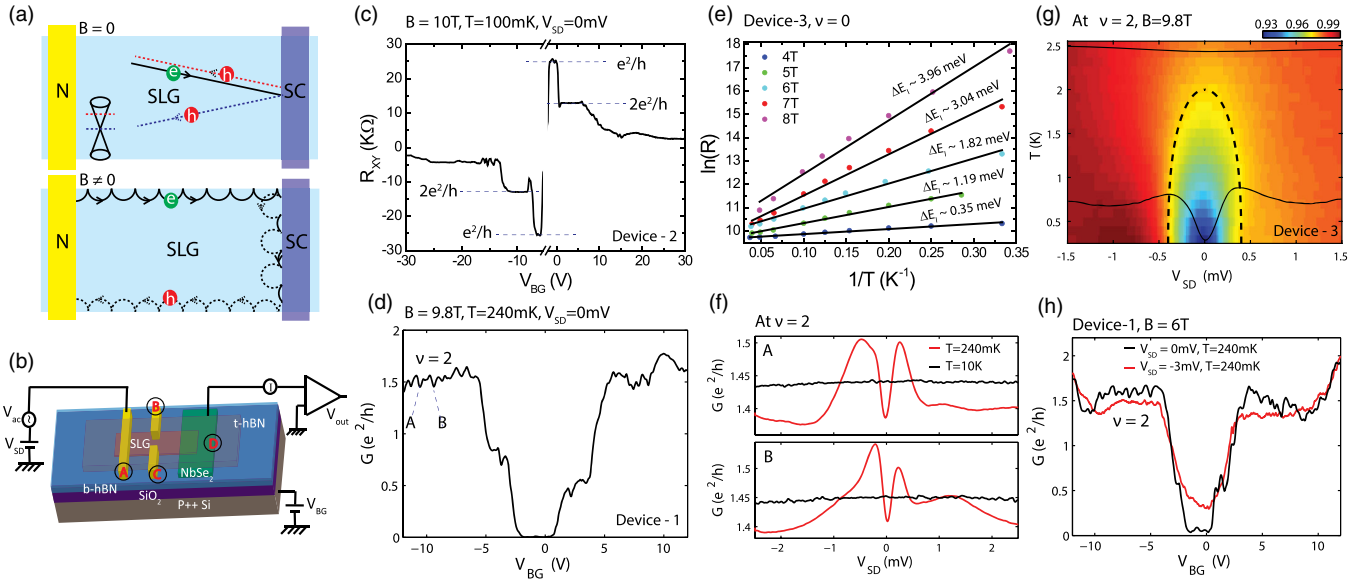

FIG. 1. (a) (top) AR in graphene at $B = 0$. The red (blue) dashed line shows retro (specular) AR. (bottom) Classical picture of AR at the interface of QH edge state and superconductor based on skipping orbit. The electron and hole orbits have the same chirality for intraband process. (b) Schematic of the experimental measurement setup of hBN protected graphene devices. For R_{xy} measurement current is injected between A and D, voltage is measured between B and C. For the two probe conductance measurement of the SLG-$NbSe_2$ junction voltage is applied at A, and the current is measured at D. (c) R_{xy} of device 2 at $B = 10$ T showing symmetry broken QH plateaus. (d) Two-terminal gate response of device 1 between Au-SLG-$NbSe_2$ at $B = 9.8$ T and $V_{SD} = 0$ mV. (e) Activation plot for device 3 at the Dirac point for different magnetic fields; the corresponding insulating gaps are shown on the figure. We note that the resistance changes by up to 3 orders of magnitude over the range of the fits. (f) dI/dV as a function of V_{SD} measured in device 1 at $B = 9.8$ T on the $\nu = 2$ LL at the positions A and B marked in (d); BCS peaks are present at 240 mK (red) but not at 10 K (black). (g) 2D color map of normalized dI/dV versus V_{SD} as a function of temperature at $B = 9.8$ T for device 3. Superconductivity vanishes at around 2 K. The black dashed line is the theoretical temperature dependence of the BCS gap. The cut lines are shown at 240 mK and 2.5 K. (h) The gate responses of device 1 for 6 T at $V_{SD} = 0$ (black) and for $|eV_{SD}| > \Delta$ (red). The former has enhanced conductance.

as a function of the back-gate voltage (V_{BG}), the source-drain bias voltage (V_{SD}), the temperature (T), and the magnetic field (B). The highest mobility of 60 000 cm^2/V sec was obtained in device 3, where the carrier inhomogeneity (δn) due to charge puddles was $\sim(3–5) \times 10^9$ cm^{-2} which corresponds to Fermi energy broadening (δE_F) of ~6–8 meV [34]. The characterization of several devices is shown in Supplemental Material, Sec. SI1 [33]. Figure 1(c) presents the Hall resistance, R_{xy}, of device 2 at $B = 10$ T, where the plateaus at $2e^2/h$ and $1e^2/h$ are clearly visible. From the B dependence of Shubnikov–de Haas oscillations [35,36] the LL broadening of $\Gamma \sim 4.5$ meV was obtained (Supplemental Material, Sec. SI3 [33]). The two-probe conductance (G) measured between SLG—superconductor contact at 9.8 T is shown in Fig. 1(d) (device 1). The value of conductance on the plateaus is lower than the ideal value due to the contact resistance of ~1.5 kΩ at the SLG-$NbSe_2$ junction. In addition to different broken symmetries, an insulating state, i.e., a $\nu = 0$ plateau, is observed at the DP as previously reported in the literature [37–41]. Using a thermally activated carrier transport model we have determined the insulating gap of the $\nu = 0$ plateau (Supplemental Material, Sec. SI5 [33]). Previous studies [40,41] have reported that the value of insulating gap of $\nu = 0$ plateau depends on Γ, and the measured activation gap is nothing but the mobility gap, $\Delta E_I = \Delta E_{LL} - \Gamma$ [36,42]. At 10 T, $\Delta E_I \sim 5$ meV was measured for device 3 (Supplemental Material, Sec. SI5 [33]), and activation plots at several B are shown in Fig. 1(e). The details of the activation plots of device 1 and device 2 are shown in the Supplemental Material, Sec. SI5 [33].

We begin by demonstrating that superconductivity in $NbSe_2$ survives up to high perpendicular magnetic fields where the uncovered graphene is comfortably in the QH regime. Figure 1(f) shows the differential conductance (dI/dV) as a function of V_{SD}, called the Andreev curve, for the values of V_{BG} marked A and B in Fig. 1(d) on the $\nu = 2$ plateau. The existence of superconductivity is evident from the BCS like conductance peaks at about ±0.5 meV for device 1 at $B = 9.8$ T. Similar features are observed for device 2 (Supplemental Material, Fig. SI4-5f and Sec. SI6 [33]). Bias spectroscopy (Supplemental Material, Sec. SI6 [33]) allows us to extract the low-T superconducting gap (2Δ) as a function of magnetic field, which we show in Fig. 4(a); the large error bars arise primarily due to the asymmetric nature of the Andreev curve (the possible origin of which is discussed below). The superconducting gap of $NbSe_2$ flake, $2\Delta \sim 2$ meV and

$T_C \sim 7$ K at 0 T was directly characterized in our previous work [Fig. 3(a) of Ref. [17]], which is consistent with the 0 T data in Fig. 4(a). Figure 1(g) shows the temperature dependence of the Andreev curves at $B = 9.8$ T, which produces a $T_c \sim 2$ K where the BCS peaks disappear. We can relate the T_c to superconducting gap through $2\Delta = 4.07 k_B T_c \sim 0.7$ meV (the factor 4.07 was determined in Ref. [43] for $NbSe_2$), which is close to that extracted from the Andreev curve at $B = 10$ T as shown in Fig. 4(a). These observations—appearance of BCS peaks in the Andreev curve [Fig. 1(f)] in a QH plateau and excellent agreement with the T dependence predicted by the BCS theory [Fig. 1(g)]—demonstrate the coexistence of the QH effect and superconductivity. It is noted that for bulk $NbSe_2$, the critical magnetic field is $H_{c2} \sim 4$–5 T [44], but surface superconductivity (H_{c3}) has been reported for up to $B =$ 7–8 T [45]; the existence of superconductivity at the interface of SLG-$NbSe_2$ at high magnetic field is thus not unexpected.

We next come to AR. Some evidence for it can be seen from the fact that the conductance at the $2e^2/h$ plateau is enhanced by ~15% [Fig. 1(h)] when V_{SD} is changed from −3 mV, where no AR is expected (because $|eV_{SD}| > \Delta$), to zero, where AR is expected. For an ideal, fully transparent contact, one expects 100% enhancement due to AR; we attribute the smaller enhancement in our system to a nonfully transparent contact. Temperature dependence of conductance enhancement at $\nu = 2$ is shown in the Supplemental Material, Fig. SI4-5g [33]. Conductance enhancement due to AR can also be seen by comparing the data below and above T_C shown in the Supplemental Material, Fig. SI4-5e [33]. We note that the change in conductance for the Andreev curve in Fig. 1(f) is around 10%. However, the change of conductance was higher ~25%–30% for device 2 in the QH regime (at $\nu = 2$ plateau) as shown in the Supplemental Material, Fig. SI6-8 [33]. At 0 T the changes in the Andreev curve were around 20% in device1 (Supplemental Material Fig. SI6-7 [33]) and 45–50% in device 2 (Supplemental Material Fig. SI6-8 [33]).

Our most important finding is shown in Fig. 2, where a closer inspection of the conductance minimum reveals, completely unexpectedly, an anomalous peak. Further investigation brings out the following properties. First, the peak is seen precisely at the DP. Second, the peak is not seen above T_C [compare Figs. 2(d) and 2(c)]. Third, its amplitude decreases with decreasing temperature as well as increasing ΔE_I, indicating that the peak is a finite temperature effect. Figure 3(a) shows the 2D color map of $\log(G)$ plotted as a function of V_{BG} and B, which displays the appearance of the peak precisely at the DP and its continuous decrement with increasing B. Finally, the parameters for which the anomalous peak is observed in device 2 and device 3 are shown by the dashed enclosed areas in the phase diagram in Fig. 4(a); for both the devices

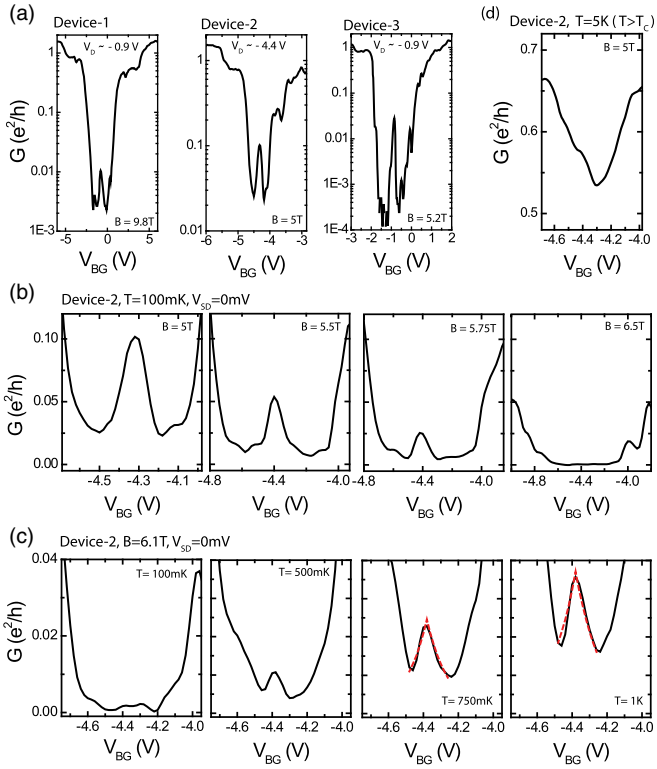

FIG. 2. (a) The anomalous conductance peak at the DP shown in several devices on a log scale. (b) The conductance peak in device 2 at different magnetic fields shows the decrement of the amplitude with increasing B. (c) The conductance peak amplitude increases with increasing temperature. The red dashed lines in the last two panels display fitting of the peak line shape with Eq. (1). (d) No conductance peak at the DP is seen for $T > T_C$.

the highlighted regime where the peak is observed satisfies the condition, $\Delta E_I < 2\Delta$.

All of these facts are naturally explained in terms of a conductance peak originating from a new mechanism, namely, finite temperature inter-Landau-level AR, in which a thermally excited electron in the $N = 0$ LL band above the E_F reflects as a hole in the $N = 0$ LL band below the E_F, as shown schematically in Fig. 4(b). Such a peak is expected to occur (i) precisely at the DP, (ii) at finite temperature but for $T < T_c$, and (iii) for $2\Delta \geq \Delta E_I$. We mention that V_{BG} at the DP depends slightly on whether the sweep is up or down, causing two different values in Fig. 2(b); in Fig. 3(a), all data are for sweep in the up direction, and show that the peak position remains invariant. We also note the presence of certain secondary, sample-specific peaks away from the DP, but their amplitudes are smaller by 2–3 orders of magnitude.

To see the activated nature of anomalous peak we plot the area under the peak in Fig. 3(b) for device 2, and fit it to a thermally activated behavior. Fitting the peak height gives a similar gap, as shown for device 3 in the inset of Fig. 3(b). Further details regarding the activation nature of the peak for all the devices are shown in Supplemental Material,

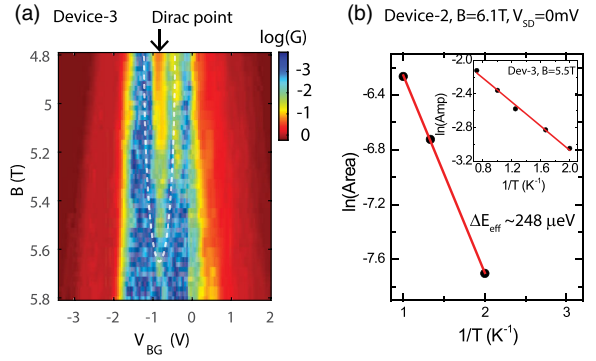

FIG. 3. (a) 2D color map of $\log(G)$ in device 3 plotted as a function of V_{BG} and B showing the presence of the anomalous peak precisely at the DP, which vanishes above 5.6 T. (b) Area of the peak plotted as a function of $1/T$ showing activated behavior with an effective gap of $\Delta E_{\rm eff} \sim 248$ μeV. In the inset, the amplitude of the conductance peak in device 3 is used to show the activated behavior, which gives $\Delta E_{\rm eff} \sim 150$ μeV.

Secs. SI8 and SI9 [33]. Fitting the area in Fig. 3(b) using $e^{-\Delta E_{\rm eff}/2k_BT}$ gives $\Delta E_{\rm eff} \sim 0.25$ meV. One may expect $\Delta E_{\rm eff}$ to be equal to the ΔE_I (mobility gap), but the former is lower by a factor of ~3. This finds a natural explanation by the fact that the temperature dependence of the resistance of SLG shows two distinct ΔE_I differing by a factor of ~3 (Supplemental Material, Sec. SI5 [33]): for example, at $B = 6$ T in device 2 for $T > 2$ K we have $\Delta E_I \sim 0.8$ meV, but for $T < 2$ K we have $\Delta E_I \sim 0.25$ meV, the latter being essentially in perfect agreement with the gap deduced from the anomalous peak at the DP. Similar results are obtained for device 3 as shown in the Supplemental Material, Sec. SI5 [33]. Although the existence of the smaller, or "soft" gap around the E_F in between the LLs at low temperature has been reported in the literature [42,46–48], its origin is not well understood. We ascribe the soft gap below 2 K to disorder.

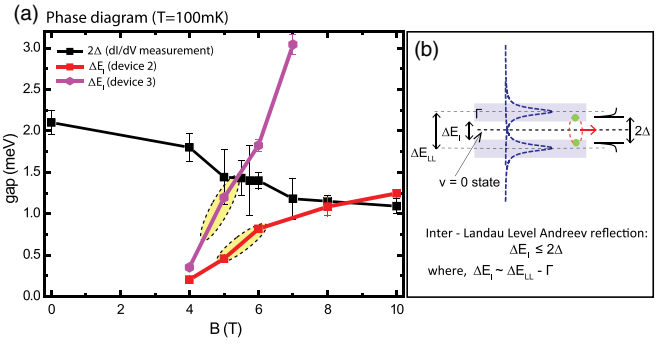

FIG. 4. (a) An experimental phase diagram in energy and magnetic field. Solid black squares are the superconducting gaps measured using bias spectroscopy as a function of B. The solid red squares and solid purple hexagons show the insulating gaps of device 2 and device 3 as a function of B, where the thick lines are a guide to the eye. The anomalous conductance peak at the DP is observed in the region enclosed by the dashed black ovals. (b) Schematic of the inter-Landau-level AR process at the DP.

To further confirm the physics of the inter-Landau-level AR we have performed extensive numerical calculations, where we consider a system of graphene in the QH regime connected to superconducting graphene. The physics of the $\nu = 0$ insulator at high B has been the subject of many studies [37,39–41,49,50] and two most likely models are in terms of a canted antiferromagnet (CAF) or an isospin ferromagnet (IFM) [30,32], the band diagrams for which are schematically shown in the insets of Figs. 5(a) and 5(b). The insulating gap of the former originates from a splitting of the $\nu = 0$ LL into Landau bands with chiral edge states, whereas for the latter it results from a coupling between the helical edge states. To keep the discussion general, we consider AR in both models. The calculated conductance as a function of chemical potential (E_F) is plotted in Figs. 5(a) and 5(b) (Supplemental Material, theory [33] for the details) for CAF and IFM, respectively. It shows a small conductance peak at the DP arising from inter-Landau-level AR [insets of Figs. 5(a) and 5(b)]. At finite temperatures, the conductance at the DP can be analytically expressed as

$$G = \frac{e^2}{h}\frac{2a}{1 + e^{[\Delta E_I/2 + |C(V_{\rm BG} - V_D)|]/k_BT}}, \qquad (1)$$

where a is the probability of AR and $C = dE_F/dV_{\rm BG}$. The experimental peak in Fig. 2(c) is fitted using the above equation with fitting parameters: $a = 0.35$, $\Delta E_I = 0.5$ meV, $C = 0.62$ meV/V for $T = 1$ K and similar fitting is also shown for $T = 0.75$ K. The fitting parameters are in general agreement with the experimental values (Supplemental Material, theory [33]).

Before ending, a comment on the physical origin of the observed asymmetry of the Andreev curves [Fig. 1(f) and Supplemental Material, Sec. SI6 [33]] is in order. dI/dV depends on the joint density of states (DOS) of the two materials. Typically, a normal metal has large and essentially constant DOS whereas the quasiparticle DOS of the superconductor is symmetric around zero bias, producing a symmetric Andreev curve. The density of states in a QH

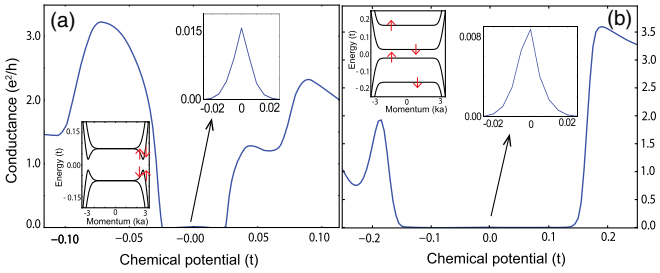

FIG. 5. Panel (a) shows numerical results based on the canted antiferromagnetic (CAF) model, and panel (b) for the isospin ferromagnet (IFM) model. The chemical potential is quoted in units of the hopping parameter t. The band diagram and the peak at the Dirac point are shown as insets.

edge, in contrast, is complicated in real materials and can be energy dependent, thus producing asymmetric Andreev curves [16,51–53]. We also note that due to the presence of the superconductor, the skipping orbits at the interface alternate between electron and hole-type orbits, whose centers are, in general, slightly offset [Fig. 1(a), bottom] [22,24], which results in an interference pattern. The fingerprints of the interference pattern can be seen as quasiperiodic conductance oscillations on the QH plateau as a function of the chemical potential [Fig. 1(h) and Supplemental Material, Sec. SI10 [33]]. We refer the reader to previous literature [16,22,24,51–55] and the Supplemental Material [33] for details.

In conclusion, our primary accomplishment is an unambiguous demonstration of AR in the graphene quantum Hall effect, which manifests most dramatically through an anomalous finite-temperature conductance peak at the Dirac point. By a combination of experimental and theoretical studies, we have confirmed its origin as thermally induced inter-Landau-level AR.

We thank Subhro Bhattacharjee, Tanmoy Das, H. R. Krishnamurthy, Subroto Mukerjee, Sumathi Rao, Sambuddha Sanyal, Ruchi Sexena, Vijay Shenoy, and Abhiram Soori for useful discussions. The authors acknowledge device fabrication and characterization facilities in CeNSE, IISc, Bangalore. A. D. thanks the Department of Science and Technology (DST), Government of India, under Grants No. DSTO1470 and No. DSTO1597. We also acknowledge the support by the U.S. Department of Energy, Office of Basic Energy Sciences, under Grant No. DE-SC0005042 (J. K. J.) and the National Key R&D Program of China (Grant No. 2016YFA0401003) and NSFC [Grant No. 11674114 (X. L.)].

*anindya@iisc.ac.in

[1] L. Fu and C. L. Kane, Phys. Rev. Lett. **100**, 096407 (2008).
[2] R. M. Lutchyn, J. D. Sau, and S. Das Sarma, Phys. Rev. Lett. **105**, 077001 (2010).
[3] Y. Oreg, G. Refael, and F. von Oppen, Phys. Rev. Lett. **105**, 177002 (2010).
[4] V. Mourik, K. Zuo, S. M. Frolov, S. Plissard, E. Bakkers, and L. Kouwenhoven, Science **336**, 1003 (2012).
[5] A. Das, Y. Ronen, Y. Most, Y. Oreg, M. Heiblum, and H. Shtrikman, Nat. Phys. **8**, 887 (2012).
[6] R. S. Mong, D. J. Clarke, J. Alicea, N. H. Lindner, P. Fendley, C. Nayak, Y. Oreg, A. Stern, E. Berg, K. Shtengel *et al.*, Phys. Rev. X **4**, 011036 (2014).
[7] J. Alicea and P. Fendley, Annu. Rev. Condens. Matter Phys. **7**, 119 (2016).
[8] D. J. Clarke, J. Alicea, and K. Shtengel, Nat. Phys. **10**, 877 (2014).
[9] K. S. Novoselov, A. K. Geim, S. V. Morozov, D. Jiang, Y. Zhang, S. V. Dubonos, I. V. Grigorieva, and A. A. Firsov, Science **306**, 666 (2004).
[10] L. Wang, I. Meric, P. Huang, Q. Gao, Y. Gao, H. Tran, T. Taniguchi, K. Watanabe, L. Campos, D. Muller *et al.*, Science **342**, 614 (2013).
[11] K. S. Kim, Y. Zhao, H. Jang, S. Y. Lee, J. M. Kim, K. S. Kim, J.-H. Ahn, P. Kim, J.-Y. Choi, and B. H. Hong, Nature (London) **457**, 706 (2009).
[12] C. W. J. Beenakker, Phys. Rev. Lett. **97**, 067007 (2006).
[13] C. Beenakker, Rev. Mod. Phys. **80**, 1337 (2008).
[14] V. E. Calado, S. Goswami, G. Nanda, M. Diez, A. R. Akhmerov, K. Watanabe, T. Taniguchi, T. M. Klapwijk, and L. M. Vandersypen, Nat. Nanotechnol. **10**, 761 (2015).
[15] M. T. Allen, O. Shtanko, I. C. Fulga, A. Akhmerov, K. Watanabe, T. Taniguchi, P. Jarillo-Herrero, L. S. Levitov, and A. Yacoby, Nat. Phys. **12**, 128 (2016).
[16] D. Efetov, L. Wang, C. Handschin, K. Efetov, J. Shuang, R. Cava, T. Taniguchi, K. Watanabe, J. Hone, C. Dean *et al.*, Nat. Phys. **12**, 328 (2016).
[17] M. R. Sahu, P. Raychaudhuri, and A. Das, Phys. Rev. B **94**, 235451 (2016).
[18] Z. Han, A. Allain, H. Arjmandi-Tash, K. Tikhonov, M. FeigelMan, B. Sacepe, and V. Bouchiat, Nat. Phys. **10**, 380 (2014).
[19] A. Soori, M. R. Sahu, A. Das, and S. Mukerjee, Phys. Rev. B **98**, 075301 (2018).
[20] W. Bishara and C. Nayak, Phys. Rev. Lett. **99**, 066401 (2007).
[21] C. Nayak, S. H. Simon, A. Stern, M. Freedman, and S. D. Sarma, Rev. Mod. Phys. **80**, 1083 (2008).
[22] H. Hoppe, U. Zülicke, and G. Schön, Phys. Rev. Lett. **84**, 1804 (2000).
[23] M. P. A. Fisher, Phys. Rev. B **49**, 14550 (1994).
[24] F. Giazotto, M. Governale, U. Zülicke, and F. Beltram, Phys. Rev. B **72**, 054518 (2005).
[25] A. Akhmerov and C. W. J. Beenakker, Phys. Rev. Lett. **98**, 157003 (2007).
[26] F. Amet, C. T. Ke, I. V. Borzenets, J. Wang, K. Watanabe, T. Taniguchi, R. S. Deacon, M. Yamamoto, Y. Bomze, S. Tarucha *et al.*, Science **352**, 966 (2016).
[27] M. B. Shalom, M. Zhu, V. Falko, A. Mishchenko, A. Kretinin, K. Novoselov, C. Woods, K. Watanabe, T. Taniguchi, A. Geim *et al.*, Nat. Phys. **12**, 318 (2016).
[28] P. Rickhaus, M. Weiss, L. Marot, and C. Schonenberger, Nano Lett. **12**, 1942 (2012).
[29] G.-H. Lee, K.-F. Huang, D. K. Efetov, D. S. Wei, S. Hart, T. Taniguchi, K. Watanabe, A. Yacoby, and P. Kim, Nat. Phys. **13**, 693 (2017).
[30] D. A. Abanin, P. A. Lee, and L. S. Levitov, Phys. Rev. Lett. **96**, 176803 (2006).
[31] P. Tikhonov, E. Shimshoni, H. A. Fertig, and G. Murthy, Phys. Rev. B **93**, 115137 (2016).
[32] M. Kharitonov, Phys. Rev. B **86**, 075450 (2012)..
[33] See Supplemental Material at http://link.aps.org/supplemental/10.1103/PhysRevLett.121.086809 for additional data on device fabrication and characterization, QH response, Andreev curves, and numerical simulation of Andreev reflection in QH regime.
[34] J. Xue, J. Sanchez-Yamagishi, D. Bulmash, P. Jacquod, A. Deshpande, K. Watanabe, T. Taniguchi, P. Jarillo-Herrero, and B. J. LeRoy, Nat. Mater. **10**, 282 (2011).

[35] X. Hong, K. Zou, and J. Zhu, Phys. Rev. B **80**, 241415 (2009).
[36] A. F. Young, C. R. Dean, L. Wang, H. Ren, P. Cadden-Zimansky, K. Watanabe, T. Taniguchi, J. Hone, K. L. Shepard, and P. Kim, Nat. Phys. **8**, 550 (2012).
[37] Y. Zhang, Z. Jiang, J. P. Small, M. S. Purewal, Y.-W. Tan, M. Fazlollahi, J. D. Chudow, J. A. Jaszczak, H. L. Stormer, and P. Kim, Phys. Rev. Lett. **96**, 136806 (2006).
[38] Z. Jiang, Y. Zhang, H. L. Stormer, and P. Kim, Phys. Rev. Lett. **99**, 106802 (2007).
[39] J. G. Checkelsky, L. Li, and N. P. Ong, Phys. Rev. Lett. **100**, 206801 (2008).
[40] X. Du, I. Skachko, F. Duerr, A. Luican, and E. Y. Andrei, Nature (London) **462**, 192 (2009).
[41] K. I. Bolotin, F. Ghahari, M. D. Shulman, H. L. Stormer, and P. Kim, Nature (London) **462**, 196 (2009).
[42] A. J. M. Giesbers, U. Zeitler, M. I. Katsnelson, L. A. Ponomarenko, T. M. Mohiuddin, and J. C. Maan, Phys. Rev. Lett. **99**, 206803 (2007).
[43] J. Rodrigo and S. Vieira, Physica (Amsterdam) **404C**, 306 (2004).
[44] X. Xi, Z. Wang, W. Zhao, J.-H. Park, K. T. Law, H. Berger, L. Forró, J. Shan, and K. F. Mak, Nat. Phys. **12**, 139 (2015).
[45] G. D'anna, P. L. Gammel, A. P. Ramirez, U. Yaron, C. S. Oglesby, E. Bucher, and D. J. Bishop, Phys. Rev. B **54**, 6583 (1996).
[46] S. Koch, R. Haug, K. Von Klitzing, and K. Ploog, Semicond. Sci. Technol. **10**, 209 (1995).
[47] A. Efros and B. Shklovskii, J. Phys. C **8**, L49 (1975).
[48] K. Bennaceur, P. Jacques, F. Portier, P. Roche, and D. C. Glattli, Phys. Rev. B **86**, 085433 (2012).
[49] A. F. Young, J. Sanchez-Yamagishi, B. Hunt, S. H. Choi, K. Watanabe, T. Taniguchi, R. Ashoori, and P. Jarillo-Herrero, Nature (London) **505**, 528 (2014).
[50] Y. J. Song, A. F. Otte, Y. Kuk, Y. Hu, D. B. Torrance, P. N. First, W. A. de Heer, H. Min, S. Adam, M. D. Stiles *et al.*, Nature (London) **467**, 185 (2010).
[51] K. Komatsu, C. Li, S. Autier-Laurent, H. Bouchiat, and S. Guéron, Phys. Rev. B **86**, 115412 (2012).
[52] G.-H. Park, M. Kim, K. Watanabe, T. Taniguchi, and H.-J. Lee, Sci. Rep. **7**, 10953 (2017).
[53] H. Takayanagi and T. Akazaki, Physica (Amsterdam) **249B**, 462 (1998).
[54] A. Morpurgo, J. Kong, C. Marcus, and H. Dai, Science **286**, 263 (1999).
[55] A. D. K. Finck, D. J. Van Harlingen, P. K. Mohseni, K. Jung, and X. Li, Phys. Rev. Lett. **110**, 126406 (2013).